PHYSICAL REVIEW A VOLUME 45, NUMBER 8 15 APRIL 1992

# Vortex morphology and Kelvin's theorem

Alain Pumir*
*Laboratory of Atomic and Solid State Physics, Cornell University, Ithaca, New York 14853-2501*

Boris I. Shraiman
*AT&T Bell Laboratories, 600 Mountain Avenue, Murray Hill, New Jersey 07974*

Eric D. Siggia
*Laboratory of Atomic and Solid State Physics, Cornell University, Ithaca, New York 14853-2501*

(Received 25 October 1991)

The Clebsch form of the Euler equations provides an intuitive picture as to how the circulation constraints direct the spatial organization of vorticity and favor the formation of vortex sheets. Porous media convection models the basic mechanism and is also the simplest generalization of the inviscid Burgers equation that allows for an incompressible velocity field. The finite time singularities of the model are studied numerically. A related convection analog to the axisymmetric Euler equations is discussed for comparison.

PACS number(s): 47.10.+g, 03.40.Gc, 47.25.Cg

The Euler equations,

$$\partial_t^2 \mathbf{x}(\mathbf{a},t) = -\partial_x p \tag{1}$$

(where $\mathbf{x}$ is the position of a fluid element with Lagrangian label $\mathbf{a}$), describe free particle motion with the constraint of incompressibility. The circulation invariants express this fact, as is seen by rewriting (1) in the form

$$\partial_t(\partial_t x_i \partial_{\mathbf{a}} x_i) = -\partial_{\mathbf{a}}[p - \tfrac{1}{2}(\partial_t x_i)^2] \tag{2}$$

from whence the consistency of the loop integral $\int \mathbf{v}\cdot d\mathbf{x}$ in Lagrangian coordinates follows (Kelvin's theorem). The natural question as to how these invariants constrain generic solutions is seldom asked because of the lack of a tractable expression in terms of the Eulerian velocity and the impracticality of Lagrangian variables.

The ideal compromise between these two descriptions, already noted in 1859 by Clebsch [1,2], is based on representing the vorticity, $\boldsymbol{\omega} = \nabla \times \mathbf{v}$, as $\nabla\lambda \times \nabla\mu$ (possible locally), which gives vortex lines a geometric interpretation as the intersection of the level surfaces of a pair of scalars $(\lambda,\mu)$. The circulation invariants then require that $\lambda,\mu$ are passively advected by the flow, and thus are Lagrangian markers. This representation is intuitively appealing since it rephrases vortex stretching as the amplification of the gradients of $\lambda,\mu$, a process generic to passive scalar advection. The dynamics of $\lambda,\mu$ is still nonlinear and to proceed further, it is very useful to exploit an analogy with convection which arises in two distinct ways. The first case, porous media convection, is obtained if we model the Euler equations, rewritten in terms of $\lambda,\mu$ by freezing the gradient of one of the scalars. Alternatively, this model is the simplest generalization of the compressible system

$$\partial_t u + u\partial_x u = 0 \tag{3}$$

to higher-dimensional incompressible flows.

The second case is axisymmetric Euler flow where an analogy with convection, this time described by the two-dimensional Boussinesq equations, occurs and in fact becomes exact, when the flow domain is a narrow shell in radius. Without this restriction, the Boussinesq equations are still a useful *model* of locally axisymmetric flow (see Ref. [3] for details).

We will show how the vortex sheets, habitually seen in Euler simulations [4,5], simply correspond to the leading, high gradient edges of thermal plumes or bubbles that intuition suggests arise very generally in buoyancy driven flows. It is just this ability to qualitatively project the evolution of general smooth initial conditions into a highly nonlinear yet organized regime that has been sorely lacking in numerical studies of vortex dynamics. We also obtain a heuristic explanation for the vorticity-strain correlations seen in the same simulations. Since we focus on these qualitative aspects, as in studies of dynamical systems, questions as to the *quantitative* validity of the porous media model, necessarily limited as to initial conditions and time of evolution, are deferred to after the numerics.

We have also pushed our simulations far enough to provide ample evidence for a finite time singularity, a subject of independent interest. While the Boussinesq model is rigorously equivalent to axisymmetric Euler when this occurs, singular solutions to the porous media equations are strictly speaking only relevant as the incompressible flow analogs to shocks in (3). As such, they may provide some formal intuition for the unconstrained Euler problem.

Any incompressible velocity field can *locally* be written in the form

$$\mathbf{v} = \mu\nabla\lambda - \nabla\phi, \tag{4}$$

where $\phi$ is fixed by incompressibility [1,6], which implies $\boldsymbol{\omega} = \nabla\lambda \times \nabla\mu$. The flux of $\boldsymbol{\omega}$ through an infinitesimal surface element is the Jacobian of $\lambda,\mu$ with respect to the two tangent directions. The advection equations for $\lambda,\mu$, defined to be canonically conjugate, may be derived from the Hamiltonian $\mathcal{H} = \frac{1}{2}\int v^2 d^3x$ (N.B. the variation of $\phi$ with respect to $\lambda,\mu$ disappears by incompressibility)

$$\partial_t\lambda + \mathbf{v}\cdot\nabla\lambda = 0, \quad \partial_t\mu + \mathbf{v}\cdot\nabla\mu = 0. \tag{5}$$

 

They are equivalent to Euler's equation in two or three dimensions. In the former case, area preservation plus the Lagrangian character of $\lambda,\mu$ requires that $\partial(\lambda,\mu)/\partial(x,y)$, which is nothing but the vorticity, is also Lagrangian so the Clebsch formulation is not particularly useful.

Imagine now that $\nabla\lambda=\hat{y}$ is frozen, then we have for $\mu$

$$\partial_t\mu+(\mu\hat{\mathbf{y}}-\nabla\phi)\cdot\nabla\mu=0. \tag{6}$$

If $\mu$ is the temperature, and the buoyancy force is linear in $\mu$, then (6) represents porous media convection because the velocity and not the acceleration equals the force. Of course, since a single velocity advects both $\lambda$ and $\mu$, the ansatz ($\nabla\lambda=\hat{y}$) is not preserved in time and the precise relation of (6) to (5) is discussed later. Equation (6) is the porous media convection model and the generalization of (3).

It is very informative to contrast (6) and (3), which is trivially solvable by transforming to Lagrangian coordinates. For sufficiently smooth initial data, (3) exhibits a universal singularity or caustic,

$$u\sim\tau^{1/2}f(x/\tau^{3/2}) \tag{7}$$

($\tau\equiv t^*-t$), which arises by inverting the variable change from Lagrangian to Eulerian coordinates. The usual physics of shock formation, implicit in (7), completely fails for (6) since there is no incompressible velocity field of the form $\mathbf{v}=(0,f(y))$. Furthermore, since (6) is not trivializable in Lagrangian coordinates, we proceed to its numerical solution in two dimensions which suffices to bring out the essential physics.

Using a Fourier code, we found, as expected, that any smooth temperature distribution evolved under (6) into a series of rising or falling plumes. To go further, an adaptive mesh code was written to follow how $\nabla\mu$ on the leading edge of a plume diverged. The entire plane was mapped into the square $|x,y|\le 1$ and second-order accurate finite differences were used in $x,y$. The point where $|\nabla\mu|$ was maximum was maintained at the origin, where the resolution was highest, by a uniform but time-dependent velocity added to (6). The developing singularity was of comparable size in $x,y$ so it was very convenient to add a time-dependent dilation to (6), $\partial_t\mu\rightarrow\partial_t\mu+\alpha\mathbf{x}\cdot\nabla\mu$, with $\alpha(t)$ chosen to keep $\int(\nabla\mu)^4d^2x$ constant. In this way, only minimal coordinate adjustments "by hand" were necessary to maintain resolution.

A $10^5$ increase in $\max|\nabla\mu|$ was observed with no impediment to further integration (Fig. 1). The fit to $t^*$ controls the height of the last peak which was placed in line with the previous two. The jump in $\mu$ across the interface may be read off from the contour plots to $\sim 20\%$ accuracy and slowly decreases. This probably accounts for the secular trend seen in $\tau|\nabla\mu|$. The shape of the interface is approximately periodic in $\ln(\tau)$ if we look modulo the local symmetries $x\leftrightarrow -x$, $y\leftrightarrow -y$, e.g., the interface can revert from concave to convex in the neighborhood of $\max|\nabla\mu|$. The other salient feature of the flow is that the interface thickness $\sigma$ and local curvature $\kappa$ maintain the relation $c_1\lesssim\kappa\sigma\lesssim c_2$ where $c_i$ are constants (Fig. 2). Since the singularity is pointlike, and the dynamics are local, many equivalent singularities would emerge elsewhere along the interface.

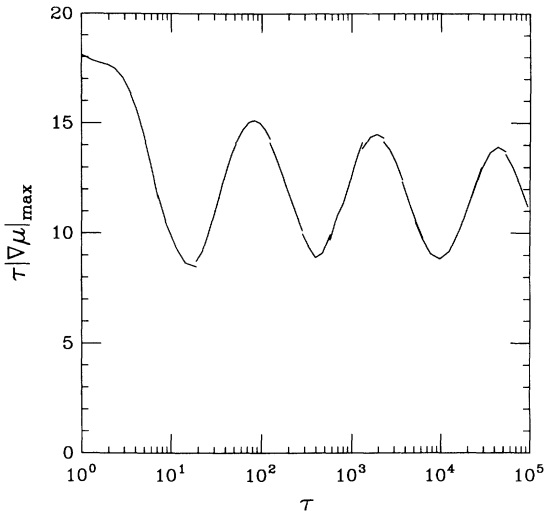


FIG. 1. The maximum $|\nabla\mu|$ vs $\tau=t^*-t$ for (6) simulated on a $256^2$ mesh. The ordinate is scaled as suggested by Eq. (8).

The regular cycles in Fig. 1 have been seen before [7], and qualitatively have a similar explanation. The $|\nabla\mu|$ grows most rapidly when $\kappa\sigma$ is largest (N.B. if the interface were flat the velocity locally would be uniform by incompressibility). By volume preservation, the compression of contour lines is accompanied by their elongation.

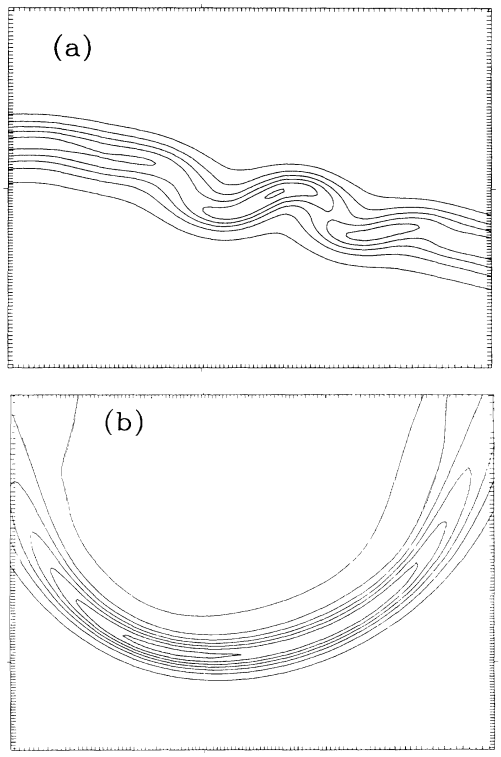


FIG. 2. Contour plots of $|\nabla\mu|$ in the vicinity of its maximum from a simulation of (6) (a) at a time corresponding to the second minima in Fig. 1 and (b) at the following maxima. The tic marks show the computational mesh.

This strain also stabilized the interface against further folds [8] until $\kappa\sigma$ has decreased appreciably and new instabilities can occur.

We can therefore plausibly write the solution to (6) as

$$\mu = \tau^{\eta} M(\mathbf{x}/\tau^{1+\eta}, \ln\tau) \tag{8}$$

with the proviso that the dependence of $M$ on its second argument be weaker than exponential. We find $\eta \simeq 0.1$ in contrast to (7), although $|\nabla\mu| \sim \tau^{-1}$ in both cases as suggested by a simple scaling treatment of the respective equations.

To derive the Boussinesq approximation for axisymmetric flow (with swirl), in a shell $r_1 \le r \le r_2$, we work in cylindrical coordinates $(r,\theta,z)$, assume $\mu(r,z)$, $\lambda = \theta + \lambda_0(r,z)$, and observe in (4) that $\phi$ is a function of $(r,z)$ only. The Hamiltonian then separates into a kinetic piece $\frac{1}{2} v_{r,z}^2$ and a (centripetal) potential piece, $\frac{1}{2} v_\theta^2 = \frac{1}{2}\mu^2/r^2$; $\mu$ and $\lambda_0$ remain canonically conjugate.

In the small $r_2/r_1 - 1$ limit, after rescalings and eliminating a term $\sim \int \mu^2 d^3r$ (a constant of the motion), the Hamiltonian becomes $\mathcal{H} = \frac{1}{2}\int (v^2 - y\mu^2)\,dx\,dy$, where $r^2 - r_1^2 \to y$, $z \to x$, and the two-dimensional (2D) velocity, $\mathbf{v}(x,y)$, obeys (4). The equations of motion for $\mu$ and the vorticity become

$$\begin{aligned} &\partial_t \mu + \mathbf{v}\cdot\nabla\mu = 0\,, \\ &\partial_t \omega + \mathbf{v}\cdot\nabla\omega = \mu\partial_x\mu\,, \end{aligned} \tag{9}$$

which describe 2D Boussinesq convection, with temperature $\mu^2/2$, suitably nondimensionalized.

The numerical results [3] for (9) (Fig. 3) may be fit by

$$\mu \sim \tau^{\eta} M(\mathbf{x}/\tau^{2+\eta}, \ln\tau),\quad \omega \sim \tau^{-1}\Omega(\mathbf{x}/\tau^{2+\eta}, \ln\tau)\,, \tag{10}$$

$\eta \sim 0.2 \pm 0.2$. The physics of the singularity is similar to (6) in that the plume tip shows Rayleigh-Taylor instability when $\kappa\sigma$ is sufficiently small but the simulation is more delicate technically. The singularity is not associated with the roll up although that does occur and may be responsible for making the dependence on $\ln\tau$ more irregular than for (6). This is most evident in the contour plots for $\mu$ and $\omega$ where one finds substantial changes in shape. Note that for (10) the three-dimensional vorticity, $\boldsymbol{\omega}$, is dominated by its $r,z$ components computed from $\nabla\mu$ (N.B. $\mu = rv_\theta$). The enstrophy is almost singular in that $\int |\omega|^{2+\epsilon} d^3r$ diverges for $\epsilon > \eta$.

Finally, what is the relevance of these two idealizations to the full three-dimensional Euler equations? The porous media model applies to those vorticity distributions for which $\nabla\lambda$ and $\nabla\mu$ vary on very different scales. The one with the most slowly varying gradient, say, $\lambda$, is frozen and defines the local direction of gravity. This condition is not as restrictive as it seems since there is a gauge freedom, $\lambda,\mu \to \lambda',\mu'$, such that $\partial(\lambda,\mu)/\partial(\lambda',\mu') = 1$, which allows any two-dimensional flow to be written as $\lambda = y$, $\mu = \int^x \omega(x',y)\,dx'$. Hence by continuity, any quasi-two-dimensional flow satisfies our criterion over a region set by the slow scale.

The correct Euler dynamics requires both $\lambda$ and $\mu$ to evolve under the same strain. When $|\nabla\lambda|$ is much greater than $|\nabla\mu|$ initially, the approximation $\nabla\lambda \sim$ const will be reasonable for some period of time. Note that under these conditions, the vorticity scales with $\nabla\mu$, so meaningful concentration and amplification can occur. At later times, some of the distortion in $\lambda$ can be removed by a gauge transformation, but in three dimensions, not all. We have been unable so far to develop any asymptotic expansion of the WKB variety to treat later times.

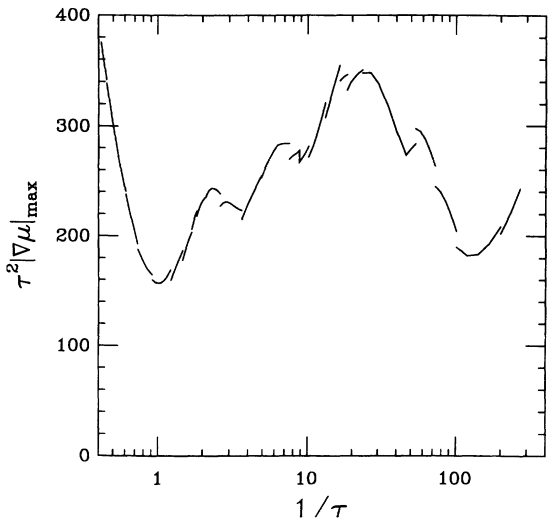


FIG. 3. The maximum "temperature" gradient for (9) (equivalent to the maximum 3D vorticity), scaled so as to remove the expected divergence [cf. Eq. (10)] vs $\tau = t^* - t$. The various extrema correlate with shape changes; the original plume first becomes unstable around $\tau \sim 0.5$–$1.0$, and for $\tau \sim 25$ the point of maximum gradient moves off the $x \to -x$ symmetry axis. The irregularities and jumps in the data are due to coordinate adjustments, and indicate the resolution errors (Ref. [3]). Note the $10^5$ increase in $|\nabla\mu|$ in the "scaling" regime.

Although largely qualitative insights into Euler dynamics, that we now recapitulate, can follow from the porous media analogy, the same intuition never emerged from direct numerical simulations. Plumes will form in three dimensions as well as two. If $\kappa\sigma$ is substantially less than one, as we have found, the three-dimensional vorticity will appear concentrated in structures that are locally sheet-like (miniature shear layers), and on a slower time scale, the sheets increase in area. This self-organization implies the unexpected vorticity-strain correlations seen in Navier-Stokes computer simulations, namely, the rate of strain matrix has one eigenvalue much smaller than the other two in magnitude with the vorticity aligned along the corresponding eigenvector [9,10].

The same conclusions follow for axisymmetric flows after we translate back from 2D Boussinesq convection to 3D vorticity. The "plume" implies a sharp jump in $\mu$, which is nothing but the conserved circulation $rv_\theta$. Since "buoyancy" is actually centripetal force, the plume tip is tangent to $r =$ const, the maximum vorticity is from $\partial_r v_\theta$ and is directed along $\hat{z}$. The dominant strain originates from the same term and is predominantly in $(r,\theta)$.

Globally, the plumes generate vortex sheets, the edges of which roll up leading to ring vortices when viewed in three dimensions. More generally, we may speculate that

the vorticity typically organizes into sheets, even without axisymmetry, which then roll up leading to the vortex filaments seen many times in Navier-Stokes simulations [9,11] and recently in experiment [12].

Analogies with convection provide an alternative picture for energy transfer in turbulence that is closer to Burgers' equation than to the usual vortex stretching ideas. The latter follow tautologically from the vorticity equation. If the strain is prescribed, this equation is linear and the vorticity can be made to assume any shape that preserves the topology. When the strain due to the vorticity is included, nothing can be said about the vortex morphology. By contrast, our models are nonlinear, yet intuitively comprehensible, and do select a generic vortex morphology. Alternatively, the Clebsch variables plus analogies with convection provide a reinterpretation of vortex stretching in terms of Burgers-like shocks.

Equation (6) in 2D is analogous to Euler in 3D since the number of spatial dimensions is one greater than the number of conserved fields, and the velocity is divergence free. Simple caustics, e.g., (7), arise generically when a finite number of scalars are transported by a velocity field than can be expressed as a $(x,t)$ independent function of the scalars. It is in this sense that (6) is not finite dimensional, and any theory for the generic singularities of the 2D area preserving maps defined by the velocity field in (6) on par with what one has for caustics, could well have important implications for the Euler equations in three dimensions.

We thank T. Dombre, N. Ercolani, and E. Titi for helpful discussions. This research was supported by the Air Force Office of Scientific Research under Grant No. AFOSR-91-0011 and the National Science Foundation under Grant No. DMR-9012974.

---

*Permanent address: Laboratoire de Physique des Statistique, Ecole Normale Supérieure, 75231 Paris, France.

[1] R. Salmon, Ann. Rev. Fluid Mech. **20**, 225 (1988).

[2] Attempts to apply the Clebsch formulation to steady-state turbulence were made by V. E. Zakharov and V. S. Lvov, Izv. Vuzov Radiofiz. **18**, 1470 (1975); and E. Levich, Phys. Lett. **87A**, 461 (1982), but this is a much more difficult problem since viscosity is required.

[3] Details are provided by A. Pumir and E. D. Siggia, Phys. Fluids (to be published).

[4] M. Brachet and M. Meneguzzi (private communication); R. Kerr (private communication).

[5] A. Pumir and E. D. Siggia, Phys. Fluids A **2**, 220 (1990).

[6] Nonzero total helicity is not an intrinsic impediment to global Clebsch variables [see E. A. Kuznetsov and A. Mikhailov, Phys. Lett. **77A**, 37 (1980)], but more complicated forms of knots in the vortex lines are.

[7] A. Pumir and E. D. Siggia, Phys. Fluids **30**, 1606 (1987).

[8] Ya. B. Zeldovich, A. G. Istratov, N. I. Kidin, and V. B. Librovich, Combust. Sci. Technol. **24**, 1 (1985); P. Pelcé and P. Clavin, Europhys. Lett. **3**, 907 (1987); G. K. Batchelor, J. Fluid Mech. **184**, 399 (1987).

[9] E. D. Siggia, J. Fluid Mech. **107**, 375 (1981).

[10] W. Ashurst, A. Kerstein, R. Kerr, and C. Gibson, Phys. Fluids **30**, 2343 (1987).

[11] A. Vincent, M. Meneguzzi, J. Fluid Mech. **225**, 1 (1991); Z. S. She, E. Jackson, and S. A. Orszag, Nature (London) **344**, 226 (1990).

[12] S. Douady, Y. Couder, and M. E. Brachet, Phys. Rev. Lett. **67**, 983 (1991).